Buletinul Ştiinţific al Universităţii "Politehnica" din Timişoara

Seria ELECTRONICĂ şi TELECOMUNICAŢII
TRANSACTIONS on ELECTRONICS and COMMUNICATIONS

Tom 49(63), Fascicola 2, 2004

Windowing Techniques for OFDM Systems

Ciprian Comşa, Florin Beldianu, Paul Cotae[1]

Abstract – Orthogonal Frequency Division Multiplexing (OFDM) is a technique which converts a frequency-selective fading channel into several nearly flat-fading channels and combats the intersymbol interferences (ISI) caused by multipath propagation. One of the problems of the OFDM technique is the inter-carrier interference (ICI) due to frequency offset and phase error. To reduce the ICI, pulse shaping and windowing techniques can be applied. To obtain an optimal windowing function, some ICI minimization criteria, as Lagrange, can be used or a numerical algorithm specific for adaptive filtering can be employed.

Keywords: OFDM, windowing, pulse shaping, inter-carrier interference, raised-cosine pulse.

I. INTRODUCTION

Orthogonal Frequency Division Multiplexing (OFDM) is a multiplexing technique which converts a frequency-selective fading channel into several nearly flat-fading channels and combats the intersymbol interferences (ISI) caused by multipath propagation. That is why it is used in some wireless communications applications, like WLAN, being included in standards as IEEE 802.11 (USA), ARIB MMAC (Japan), HIPERLAN/2 (ETSI BRAN Europe). Also OFDM is employed for Digital Audio Broadcast (DAB) applications and known as Digital Multitone (DMT) for broadband wireline communication systems, namely high-bit-rate / asymmetric digital subscribers line (HDSL / ADSL).

Advantages of OFDM are that it is bandwidth ff t nd that it is rather insensitive to fre uenc selective fading and timing offset. The most important disadvantage though is that OFDM is sensitive to carrier frequency offset (CFO). Hence, OFDM is sensitive to frequency offset which leads to intercarrier interferences (ICI) and hence performance degradation. This kind of performance degradation and techniques for estimating the frequency offset was discussed in some references [9], [10], [13]. The use of pulse shaping to reduce the sensitivity of OFDM systems to frequency offset is examined [1]-[3], [10]-[12], while another new windowing functions for OFDM are reported [7]. Instead of g, ventional filterin_ techni ues may be used to reduce the out-of-band spectrum. Windowing and filtering are dual techniques: multiplying an OFDM symbol by an window means the spectrum is going to be a convolution of the window function with a set of impulses at the subcarrier frequencies. Applying filtering, a convolution is done in the time domain and the OFDM spectrum is multiplied by the frequency response of the filter. When using filtering, extracare has to be taken not to introduce too much rippling effects on the envelope of the OFDM symbols. Also, digital filtering implementation is much more complex than windowing [13].

This paper analysis the performance enhancements expressed in ICI power brought by the use of some types of pulses in pulse shaping and windowing functions and compares the results, looking for an optimal windowing function. In order to obtain this, some ICI minimization criteria, as Lagrange, can be used or a numerical algorithm specific for adaptive filtering can be employed.

II. SYSTEM MODEL

In order to give a mathematical description [4], [5] of an OFDM system we assume a system with N subcarriers, a bandwidth of B Hz and an OFDM symbol length of T_S seconds, of which T_{CP} is the length of the cyclic prefix. The spacing between subcarriers is given by (1), as shown in Fig. 1.

$$T = \frac{1}{\Delta f} = \frac{N}{B} = T_S - T_{CP} \qquad (1)$$

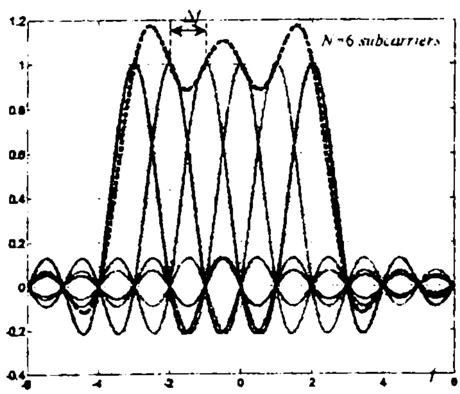

Fig. 1. Subcarriers of an OFDM system.

[1] "Gh. Asachi" Technical University of Iaşi, Telecommunications Department, 11 Carol I Blvd., Iaşi, 700506, Romania, e-mail: ccomsa@etc.tuiasi.ro

Fig. 2 illustrates the baseband OFDM model mathematically described bellow [4], [5]. Every n^{th} OFDM symbol of the transmission stream can be written as a set of modulated carriers transmitted in parallel. Relations (2) express the waveforms used in modulation.

$$\phi_k(t) = \begin{cases} \frac{1}{\sqrt{T_S - T_{CP}}} \cdot e^{j2\pi f_k (t - T_{CP})} & , t \in [0, T_S) \\ 0 & , \text{otherwise} \end{cases}, \text{ where}$$

$$f_k = f_C + \left(k - \frac{N-1}{2}\right)\cdot\frac{1}{T}, \quad k = 0,\ldots,N-1, \text{ for passband or} \quad (2)$$

$$f_k = \frac{k}{T}, \quad k = 0,\ldots,N-1, \text{ for baseband echivalent}$$

Note that nonzero term of $\phi_k(t)$ has the period $[T_{CP}, T_S)$ and $\phi_k(t)$ has a common part (3).

$$\phi_k(t) = \phi_k(t + \frac{N}{B}), \quad \text{for } t \in [0, T_{CP}) \qquad (3)$$

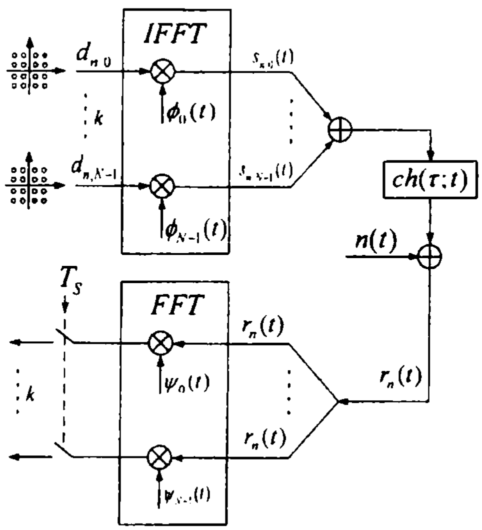

Fig. 2. Baseband OFDM system model.

If $d_{n,0},\ldots,d_{n,N-1}$ denotes the complex symbols, obtained by QAM mapping of the input data stream, the n^{th} OFDM symbol $s_n(t)$ is expressed by (4) and the infinite sequence of OFDM symbols transmitted is obtained by juxtaposition of the individual ones.

$$s(t) = \sum_{n=-\infty}^{\infty} s_n(t) = \sum_{n=-\infty}^{\infty}\sum_{k=0}^{N-1} d_{k,n}\phi_k(t - nT_S) \quad (4)$$

Assuming the impulse response $ch(\tau;t)$ of the physical channel (possibly time variant) is restricted to the length of cyclic prefix $\tau \in [0, T_{CP})$, the received signal becomes (5), where $n(t)$ is the complex, additive and white Gaussian (AWGN) channel noise.

$$r(t) = (ch * s)(t) = \int_0^{T_{CP}} ch(\tau;t)s(t-\tau) + n(t) \quad (5)$$

The filter from the receiver is matched to the last part $[T_{CP}, T_S)$ of the transmitter waveform (6), the CP being this way effectively removed in the receiver. Since the cyclic prefix contains the ISI, the sample output from the receiver filter bank contains no ISI. Also, we can ignore the time index n when calculating the sampled output at the k^{th} matched filter (7).

$$\psi_k(t) = \begin{cases} \phi_k^*(T_S - t) & , t \in [0, T_S - T_{CP}) \\ 0 & , \text{otherwise} \end{cases} \qquad (6)$$

$$e_k = (r * \psi_k)(t)\big|_{t=T_S} = \int_{-\infty}^{\infty} r(t)\cdot\psi_k(T_S - t)\cdot dt \quad (7)$$

Considering the channel to be fixed over the OFDM symbol interval, denoting it by $ch(\tau)$ and taking into account the orthogonality condition expressed by (8), we obtain after some mathematical operations the output data, given by (9).

$$\int_{T_{CP}}^{T} \phi_l(t)\cdot\phi_k^*(t) = \delta(k-l) \qquad (8)$$

$$e_k = h_k \cdot d_k + n_k, \quad \text{where}$$

$$h_k = \int_0^{T_{CP}} ch(\tau)\cdot e^{-j2\pi k\tau\frac{B}{N}}\cdot d\tau \text{ and} \qquad (9)$$

$$n_k = \int_{T_{CP}}^{T_S} n(T_S - t)\cdot\phi_k^*(t)\cdot dt$$

By sampling the low-pass equivalent signal of (2) and (4) at a rate N times higher than the subcarrier symbol rate $1/T$, we can obtain the discrete model of the baseband OFDM system, where the modulation/demodulation with waves ϕ/ψ can be replaced with iDFT/DFT (or practically with IFFT/FFT) and the channel model with discrete-time convolution.

An OFDM symbol can be constructed as follows [4], [6]. First, the data to be transmitted is mapped to a complex value X_k in the frequency domain, according to a QAM signal constellation. Second, the IDFT is calculated, normally using an IFFT algorithm, to get a complex time domain OFDM symbol

$$x_n = IFFT\{X_k\} = \frac{1}{\sqrt{N}}\sum_{k=0}^{N-1} X_k e^{-j\frac{2\pi kn}{N}} \qquad (10)$$

where N is the number of subcarriers. To make OFDM more robust against multipath and timing offset, each symbol is extended with a cyclic prefix (CP). The CP is constructed by copying the last N_g samples of the OFDM symbol (T_{es} being the sampling period) at the beginning of it. So, the OFDM symbol transmitted is $x_{-N_g}\ x_{-N_g+1} \ldots\ldots x_{N-2}\ x_{N-1}$. Finally, the time domain signals are D-A converted, mixed with a carrier, filtered and transmitted through the air. In the receiver, the opposite operations are performed using A-D conversion and DFT calculation.

III. PULSE SHAPING AND WINDOWING

The complex envelope of one N-subcarrier OFDM block with pulse-shaping is expressed as (11), where $j = \sqrt{-1}$, f_c is the carrier frequency, f_k is the subcarrier frequency of the k-th subcarrier, $p(t)$ is the time-limited pulse shaping function and $a_k, k=0,1,\ldots,N-1$ is a complex-valued data symbol transmitted on the k-th subcarrier.

$$x(t)=e^{j2\pi f_c t}\cdot\sum_{k=0}^{N-1}a_k p(t)e^{j2\pi f_k t} \quad (11)$$

Equation (12) expresses the condition that the Fourier transform of the pulse $p(t)$ should have spectral nulls at the frequencies $\pm 1/T$, $\pm 2/T$, to ensure subcarrier orthogonality [8].

$$\int_{-\infty}^{\infty} p(t)e^{j2\pi(f_k-f_m)t}dt=\begin{cases}1 & , \quad k=m\\ 0 & , \quad k\neq m\end{cases} \quad (12)$$

$$f_k-f_m=\frac{k-m}{T} \quad (13)$$

There are considered here three time-limited-pulses, which are $P_r(f)$, $P_{rc}(f)$ and $P_{btrc}(f)$ denoting the rectangular pulse, the raised-cosine pulse (in the time-domain) and the "better than" raised cosine (BTRC) pulse (in the time-domain), defined as (14), (15) and (16), where α is the roll-off factor and $0\le\alpha\le 1$ [12]. When $\alpha=0$ both raised-cosine and the BTRC pulse coalesce into the rectangular pulse. The Fourier transforms are denoted by $P_r(f)$, $P_{rc}(f)$ and $P_{btrc}(f)$ respectively. Fig. 3 shows the frequency functions of these pulses for $\alpha=0.2$ and $\alpha=1$.

$$p_r(t)=\begin{cases}1/T & , \quad -T/2\le|t|\le T/2\\ 0 & , \quad \text{otherwise}\end{cases} \quad (14)$$

$$p_{rc}=\begin{cases}\frac{1}{T} & 0\le|t|\le\frac{T(1-\alpha)}{2}\\ \frac{1}{2T}\left(1+\cos\left(\frac{\pi}{\alpha T}\left(|t|-\frac{T(1-\alpha)}{2}\right)\right)\right) & , \quad \frac{T(1-\alpha)}{2}\le|t|\le\frac{T(1+\alpha)}{2}\\ 0 & \text{otherwise}\end{cases} \quad (15)$$

$$p_{btrc}(t)=\begin{cases}\frac{1}{T} & , \quad 0\le|t|\le\frac{T(1-\alpha)}{2}\\ \frac{1}{T}e^{\frac{-2\ln 2}{\alpha T}\left(|t|-\frac{T(1-\alpha)}{2}\right)} & \frac{T(1-\alpha)}{2}\le|t|\le\frac{T}{2}\\ \frac{1}{T}\left(1-e^{\frac{-2\ln 2}{\alpha T}\left(\frac{T(1+\alpha)}{2}-|t|\right)}\right) & , \quad \frac{T}{2}\le|t|\le\frac{T(1+\alpha)}{2}\\ 0 & \text{otherwise}\end{cases} \quad (16)$$

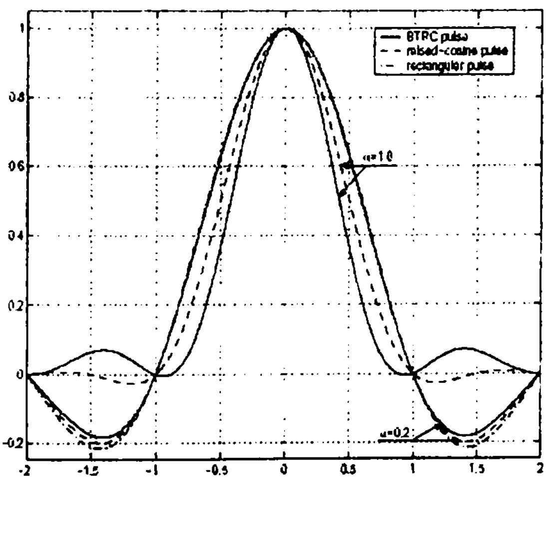

Fig. 3. Frequency functions $P_r(f)$, $P_{rc}(f)$ and $P_{btrc}(f)$.

Another family of pulses has recently been reported [11], than are intersymbol interference-free. It is about conjugate root pulses, which are not linear phase, whereas the root raised-cosine (RC) pulses are linear phase. The first-order conjugate-root pulse phase is piecewise linear, while the fourth-order pulse phase is not piecewise linear. First-order conjugate-pulses are expressible in the time domain in closed-form (17), while fourth-order pulses have more complicated forms. Both first-order conjugate-pulses and fourth-order pulses together with root raised-cosine pulses are plotted in the time domain for $\alpha=0.35$ in Fig. 4.

$$p(t)=\frac{\sin\left(\frac{\pi t}{T_{es}}\right)\cos\left(\frac{\alpha\pi t}{T_{es}}\right)}{\left(\frac{\pi t}{T_{es}}\right)(2\alpha t+T_{es})} \quad (17)$$

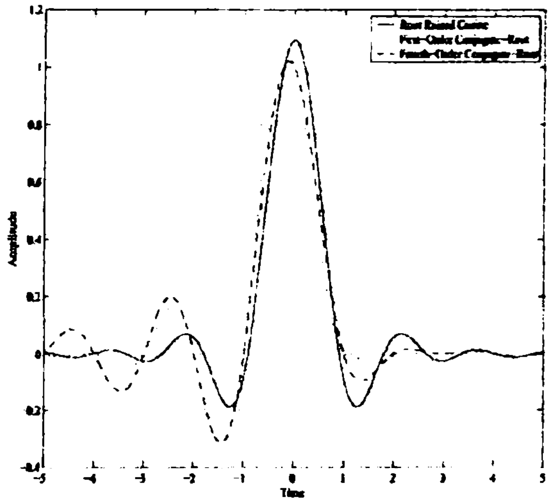

Fig. 4. Time-domain plots of the RC and conjugate-root pulses for $\alpha=0.35$

IV. PERFORMANCES OF PULSE SHAPING

Frequency offset, $\Delta f\ (\Delta f\ge 0)$, and phase error, θ, are introduced during transmission because channel distortion or receiver crystal oscillator inaccuracy. The received signal after multiplication by $e^{j(2\pi(-f_c+\Delta f)t+\theta)}$ becomes (18).

$$r(t)=e^{j(2\pi\Delta f t+\theta)}\sum_{k=0}^{N-1}a_k p(t)e^{j2\pi f_k t} \quad (18)$$

$$\hat{a}_m=\int_{-\infty}^{\infty}r(t)e^{-j2\pi f_m t}dt=$$
$$=a_m e^{j\theta}\int_{-\infty}^{\infty}p(t)e^{j2\pi\Delta f t}dt+ \quad (19)$$
$$+e^{j\theta}\sum_{\substack{k=0\\k\neq m}}^{N-1}a_k\int_{-\infty}^{\infty}p(t)e^{j2\pi(f_k-f_m+\Delta f)t}dt$$

The m-th subchanel correlation demodulator, thus, gives the decision variable for transmitted symbol a_m in (19), where the first term contains the desired signal component, and the second term is the ICI. Combining (13) with (19) gives (20), where $P(f)$ is the Fourier transform of $p(t)$. Hence, the power of the desired signal is (21) and the ICI power is (22).

$$\hat{a}_m = a_m e^{j\theta} P(-\Delta f) + e^{j\theta} \sum_{\substack{k=0 \\ k \neq m}}^{N-1} a_k P\left(\frac{m-k}{T} - \Delta f\right) \quad (20)$$

$$\sigma_m = |a_m|^2 |P(\Delta f)|^2 \quad (21)$$

$$\sigma_{ICI}^m = \sum_{\substack{k=0 \\ k \neq m}}^{N-1} \sum_{\substack{n=0 \\ n \neq m}}^{N-1} a_k a_n^* P\left(\frac{k-m}{T} + \Delta f\right) P\left(\frac{n-m}{T} + \Delta f\right) \quad (22)$$

The ICI power depends not only on the desired symbol location, m, and the transmitted symbol sequence, but also on the pulse-shaping function and the number of subcarriers. However, (22) gives the average ICI power, averaged across different sequences as

$$\overline{\sigma_{ICI}^m} = \sum_{\substack{k=0 \\ k \neq m}}^{N-1} \left| P\left(\frac{k-m}{T} + \Delta f\right) \right|^2 \quad (23)$$

For the same value of α the BTRC pulse outperforms the others, including raised cosine (RC) pulse, as shown in Fig. 5 for $\alpha = 1$ [12]. This interesting behavior occurs despite the fact that the tails of $P_{btrc}(f)$ and $P_{rc}(f)$ decay as f^{-2} and f^{-3}, respectively.

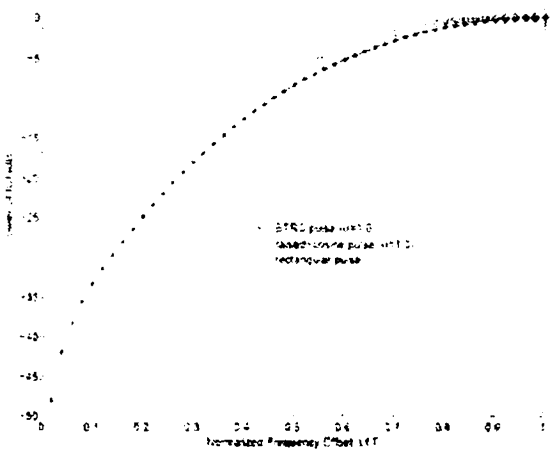

Fig. 5. The ICI power for different pulse shaping functions.

One can also consider the comparative performances of different pulses in terms of the average signal power to average ICI power ratio, denoted SIR. It will be shown that the BTRC pulse also outperforms the other pulses considered.

V. CONCLUSIONS

This paper analyzed the performance enhancements expressed in ICI power brought by the use of some types of pulses and it concluded that the employment of the "better than" raised-cosine pulse rather than the raised-cosine pulse gives a substantial improvement in the reduction of ICI caused by frequency offset in an OFDM system. However, further work has to be done in comparison those pulse shapes with another windowing functions, reported to the distortion introduced and to the implementation complexity. Also, another pulse shapes may be found using a method of parametric construction of ISI-free pulses, based on some optimization criteria (as Lagrange method) of some properties of interest, like ICI.

REFERENCES

[1] Beaulieu N. C. and Cheng J., *Precise error rate analysis of bandwidth efficient BPSK in Nakagami fading and co-channel interference*, IEEE Trans. Communications., vol. 52, pp. 149–158, Jan. 2004.

[2] Beaulieu N. C. and Damen M. O., *A parametric construction of ISI-free pulses*, Proc. of 8th Canadian Workshop on Information Theory, 2003, pp. 121-124

[3] Beaulieu N. C., Tan Ch. C., Damen M. O., *A "Better Than" Nyquist Pulse*, IEEE Communications Letters, Vol. 5, No. 9, September 2001

[4] Comşa C. R., Bogdan I., *System Level Design of Baseband OFDM for Wireless LAN*, International Symposium on Signals, Circuits and Systems, July 10-11, Iaşi, 2003, Proceedings, pp. 313-316

[5] Edfors O., Sandell M., Van de Beek J. J., *An Introduction to Orthogonal Frequency-Division Multiplexing*, 1996

[6] Intini A. L., *Orthogonal Frequency Division Multiplexing for Wireless Networks*, Santa Clara University of California, 2000

[7] Lawrey E. Ph., *Adaptive Techniques for Multiuser OFDM*, Thesis submitted in December 2001 for the degree of PhD, James Cook University, Australia

[8] Proakis J. G., Salehi M., *Communication Systems Engineering - Second Edition*, Prentice Hall, 2002

[9] Ramasami Vijaya Chandran, *Orthogonal Frequency Division Multiplexing*, University of Kansas, USA, May 2001

[10] Sun Yi, *Bandwidth-Efficient Wireless OFDM*, IEEE Journal on Selected Areas in Communications, vol. 19, no. 11, Nov. 2001

[11] Tan Ch. C., Beaulieu N. C., *Transmission Properties of Conjugate-Root Pulses*, IEEE Transactions on Communications, Vol. 52, No. 4, April 2004

[12] Tan P., Beaulieu N. C., *Reduced ICI in OFDM Systems Using the "Better Than" Raised-Cosine Pulse*, IEEE Communications Letters, Vol. 8, No. 3, March 2004

[13] Van Nee R. and Prasad R., *OFDM for Wireless Multimedia Communications*, Artech House Publishers, Boston, 2000